The Journal of the Oceanological Society of Korea
Vol. 26, No. 1, pp. 1-12, March 1991

A Geophysical Study of a Deep Sea Basin Southeast of the Hawaiian Island : Gravity, Magnetic, and Seismic Profiling

MAN CHEOL SUH*, CHAN HONG PARK**, HEE OK JUNG†, CHANG RYUL KIM**, BONG CHOOL SUK**, AND JUNG KEUK KANG††

Dept. of Geological Science, Kongju National University, Kongju, 314-110, Korea
***Marine Geophysics Lab., KORDI, Ansan, Kyongkido 425-600, Korea*
†Dept. of Ocean Engineering, Kunsan National University, Kunsan 573-600, Korea
††Lab. of Marine Mineral Resources, KORDI, Ansan, Kyongkido 425-600, Korea

Hawaii 동남부 심해저 분지에 대한 지구물리학적 연구 : 중력, 자력 및 탄성파 탐사

서만철* · 박찬홍** · 정희옥† · 김창렬** · 석봉출** · 강정극††

*공주대학교 지질과학과
**한국해양연구소 해양지구물리연구실
†군산대학교 해양공학과, ††한국해양연구소 광물자원연구실

A multi-disciplinary geophysical study including gravity, magnetic, and seismic reflection profiling was carried out in the area between the Clarion fracture zone and the Clippertone fracture zone of the northeastern equatorial Pacific basin. There are small free-air gravity anomalies of less than 20 mgal over seamounts and the east-west trending abyssal hills. The negative residual gravity anomalies over seamounts may indicate the existence of low density seamount roots compared to surrounding oceanic crust.

Non-existence of magnetic lineations and the magnetic anomalies of small amplitude with no polarity change in the east-west direction support that the study area belongs to the Cretaceous magnetic quiet zone. Positive magnetic anomalies over seamounts offset 100 km in the east-west direction in the southern part of the study area suggest a possibility of left-lateral movement of those seamounts along unknown fractures.

The sedimentary section in the study area can be divided into three units (Unit I, Unit IIA, and Unit IIB) on the basis of reflection characteristics. The total thickness of sedimentary section varies from 200 to 400 meters and the sedimentary section is thicker in the southern area of rough topography near the seamount belt than in the northern flat area. Manganese nodules are abundant in the southern part of the study area where the ridges are developed and the Unit I layer is thicker than 100 meters.

적도 북동 태평양 클래리언-클리퍼톤 변환단층대 사이의 망간탐사 구역에 대하여 중력, 자력 및 탄성파탐사를 포함한 종합적인 지구물리탐사가 수행되었다. 해저면에 발달된 해저산이나 동서방향의 해저구릉들은 최고 20 mgal의 양의 Free-air 중력 이상을 보여준다. 해산부근에서의 음의 Bouguer 및 Residual 중력이상치는 해산하부에 주위의 해양지각보다 낮은 밀도의 암석이 존재함을 시사한다.

자력이상대가 발견되지 않는 사실과 동서방향의 극성변화없는 미약한 자력이상치는 본 조사지역이 백악기말의 Magnetic Quiet Zone에 속함을 의미하며 또 남쪽 조사구역의 동서방향으로 100 km 이상 떨어진 해산들에서 공통적으로 발견되는 양의 자기이상치는 이들 해산들이 발견되지 않은 단층대를 따라 좌향이동 되었을 가능성을 보여준다.

조사구역내의 퇴적암층은 태평양 분지내 다른 지역과 동일한 탄성파 반사특성을 보이며 세 층으로

나누어진다. 퇴적암층은 약 200-400 m의 두께를 보이며, 해산 등의 험한 해저지형을 갖는 남쪽이 평탄한 북쪽보다 두꺼운 퇴적층을 보인다. 망간단괴들은 남쪽지역의 해산이 발달되고 Unit I의 두께가 100 m 이상되는 지역에 가장 많이 분포한다.

INTRODUCTION

The Exclusive Economic Zone (EEZ) in the Central Pacific has been explored intensively for the exploration of manganese nodules by nations such as U.S.A., U.S.S.R., France, England, and Japan (Andrews *et al.*, 1984 ; Calvert *et al.*, 1978). The Korea Ocean Research and Development Institute (KORDI), in cooperation with the U.S. Geological Survey (USGS), has conducted a multi-disciplinary study of manganese nodules distribution in a area bounded by Clarion and Clipperton fracture zones (C-C Zone) of the northeastern Equatorial Pacific Ocean.

The study area is located approximately 780 km southeast of Hawaii in the westernmost section of the Pacific plate which is tectonically inactive (Fig. 1). The bathymetry map (Fig. 2) shows a characteristic seafloor morphology in the area. Contour lines are generally parallel to the Clarion and Clippertone fracture zones having a WSW-ENE trend (Fig. 2). The seafloor does not show such an apparent abyssal hill topography as the Gloria images around Hawaii. The abyssal hills and the seamounts have reliefs of about 1300 m and are mostly located in the southern part of the study area (Fig. 2).

Multi-disciplinary geophysical exploration, including air-gun seismic reflection profiling, 3.5 kHz subbottom profiling, 10.2 kHz bathymetry surveying, and gravity ad magnetic measurements, was conducted in a 55500 km^2 tract as a reconnaissance study for the manganese exploration project which is now being conducted by KORDI. The track lines for the air-gun seismic profiling were laid out to cross the major topographic features at nearly right angles (Fig. 2). Although the orientation of those track lines would result in poor resolution of any anomalies associated with seafloor spreading, the major objective of the survey was to study morphological characteristics which may affect the formation and distribution of manganese nodules. In this paper, results of seismic

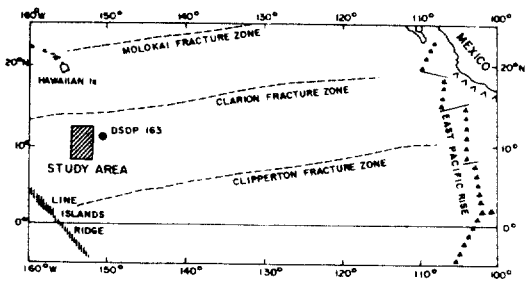

Fig. 1. Tectonic map of the area surrounding the study area.

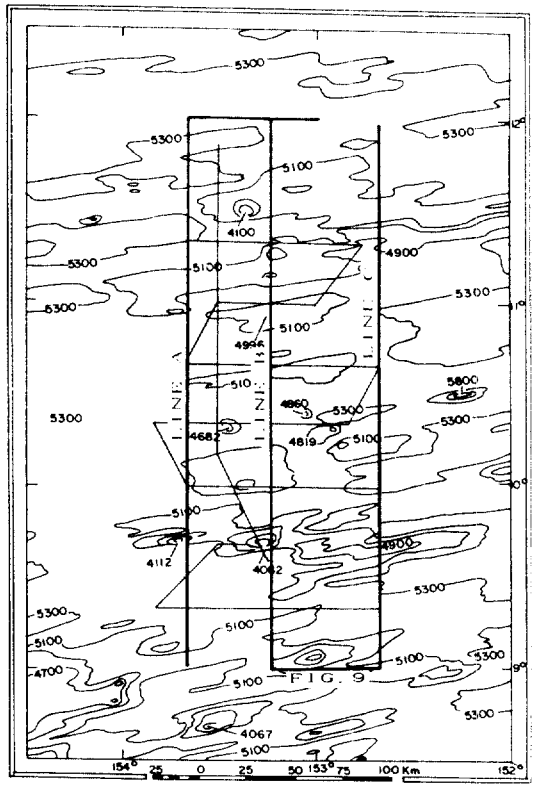

Fig. 2. Geophysical survey track lines are shown on bathymetry contours in meter. The solid lines are the tracks where the air-gun seismic survey was done together with gravity and magnetic data collection.

reflection, gravity, and magnetic studies are presented.

TECTONIC SETTING OF THE STUDY AREA

The tectonic position of the area, located about 1000 km east of the Line Islands, is somewhat unclear. Many researchers (Larson *et al.*, 1972; Winterer *et al.*, 1973 and Winterer, 1976) have studied the tectonic evolution of the area. However, there are still many uncertainties about its tectonic evolution. Examination of the models suggested by all the different researchers is beyond the scope of this study. We will summarize the sequence of tectonic events speculated by Winterer (1976). Only the events occurring later than 115 Ma will be discussed to show the age relationships between the study area and the surrounding geological structures.

A tectonic map of the area is shown in Fig. 1. According to Winterer (1976), the Pacific and the Farallon plates were separated by a ridge at the present-day location of the Line Island chain about 110 Ma. Assuming the Line Island chain is a relict of the Pacific-Farallon spreading ridge, Winterer infered the age of the island chain as 100-115 My. The Line Island chain is not orthogonal to the C-C fracture zones. This geometrical relationship requires a change of orientation of the ridge axis sometime in the 10 My after the formation of the Line Islands to a direction more nearly orthogonal to the fracture zones. The Pacific-Farallon ridge, then, jumped eastward to the present-day location of our study area between 105 Ma and 75 Ma. The age of the oceanic crust at DSDP site 163, about 100 km east of the study area has been estimated to be 78 My by Van Andel and Heath (1973). The age of the oceanic crust of the study area can be therefore considered to be slightly older than 80 My.

The morphology of ocean floor will be discussed in relation to the sediment thickness. The area is characterized by elongated ridges nearly parallel to the C-C fracture zones. In a few places in the south, the trend of ridges appear to be offset in a left-lateral sense along the northeast-trending faults. The offset seems to be related to the unnamed fracture zone proposed by Sclater *et al.* (1971). The unnamed fracture zone is within 50′ in latitude to the south of our study area. The offset may be a result of shear stress within an area between transform faults. In contrast to the south half of the survey area, where several seamounts reach up to about 4000 m below sea level, the northern half is characterized by nearly flat basin with relief less than 200 m (except for one seamount in the northwestern corner).

DATA ACQUISITION AND PROCESSING

Shipboard navigation included GPS and Loran C with a FARNAV integrated navigation system aboard the Farnella. GPS was available for approximately 13 hours per day during the entire survey. Seismic reflection data were acquired using two 40 in^3 air-guns and a Teledyne two-channel streamer along the tracks of 11136 km in total length. The ship speed was maintained at about 7.5 knots and the air-guns were fired every 9 seconds (35 m spacing). Seismic reflection data were recorded for all frequency bands using two Raytheon line scan recorders with different vertical exaggerations for the intervals of 4-8 seconds or 4.4-8.4 seconds depending on bathymetry.

Gravity and magnetic field were measured every 20 seconds using the LaCoste-Romberg Sea Gravimeter (Model S-53) and a proton precession magnetometer (Geometrics Model G801) along 7789 km of the cruise track. Measured gravity data were processed by subtraction of a reference value, Eötvös correction and low pass filtering to get Free-air gravity anomalies. The free-air gravity anomalies were converted into Bouguer anomaly by subtraction of the gravity effect of mass deficiency of sea water using the equation $dg_B = dg_{FA} - 41.97 \rho h$ where ρ is density contrast between sea water and seamount (g/cm^3), h is depth in km, dg_B is the Bouguer anomaly (mgal), and dg_{FA} is free-air gravity anomaly (mgal). The density contrast used in this study was $-1.67\ g/cm^3$ assuming that the

densities of sea water and seamount are 1.03 g/cm^3 and 2.7 g/cm^3, respectively.

Free-air gravity data were contoured in an interval of 10 mgal. The study of crossover errors (COE), the difference in gravity values at the crossings of two tracks, indicates that there are about 15 mgals of COEs. Considering a standard deviation of 22.43 mgal of crossover errors based on more than 63000 COEs of worldwide marine gravity data set (Wessel and Watts, 1988), our data set is of average quality. Gravity data from some tracks with COEs bigger than 10 mgal were not used in contouring because the variation of gravity anomaly is small in the study area.

Total magnetic intensity data were reduced to magnetic anomalies by removing the regional field calculated using the IGRF 1980 from the measured total magnetic intensities. Measurement of the diurnal variations of the geomagnetic fields was not attempted during this survey. In general, diurnal variations show errors up to +/− 30 gamma from the measured anomaly. Therefore, the magnectic anomaly of the study area can have the maximum errors of about 30 percent.

GRAVITY

North-south profiles of gravity and magnetic anomalies are shown together with morphology in Fig. 3. All the seamounts are well-correlated with local free-air gravity highs of up to 35 mgal. In general, local gravity high zones are wider than seamounts due to their deep positions. The profiles of simple Bouguer anomaly show lower values of Bouguer anomaly on seamounts than those on flat areas nearby, giving negative residual anomalies as low as −70 mgal (Fig. 3). This may indicate the existence of low density material beneath seamounts even though topographic correction was not conducted. Topographic corrections for seamounts would result in decreasing of the amplitude of Bouguer anomalies and residual anomalies over the seamounts. Gravity modeling would be helpful to resolve the low density material beneath seamounts.

The Free-air gravity anomaly has relatively low

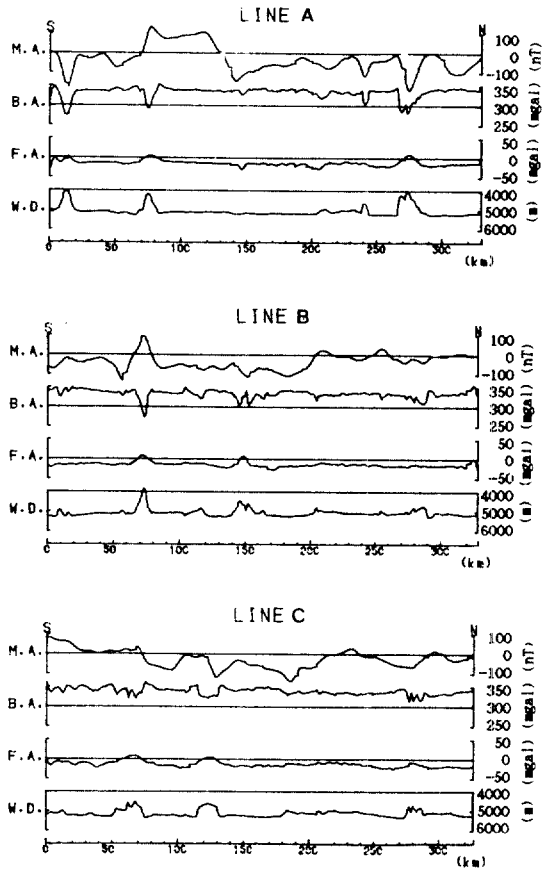

Fig. 3. Profiles of gravity and magnetic anomalies with bathymetry (WD: water depth, FA: free-air gravity anomaly, BA: Bouguer gravity anomaly, MA: Magnetic anomaly).

values ranging from −36 to 19 mgal in the study area (Fig. 4). A positive anomaly belt of less than 10 mgal, trending east-west, is found near 9°40′N. This positive anomaly belt is interpreted to be a gravitational expression of a seamount belt which has relief of about 500-1100 m. Another positive anomaly belt in the northern part of the study area is also related to an abyssal hill belt. Isolated circular positive anomaly zones of about 10 mgal represent existance of isolated seamounts.

MAGNETICS

Fig. 5 displays amplitude of magnetic anomalies plotted in a coordinate normal to the survey lines.

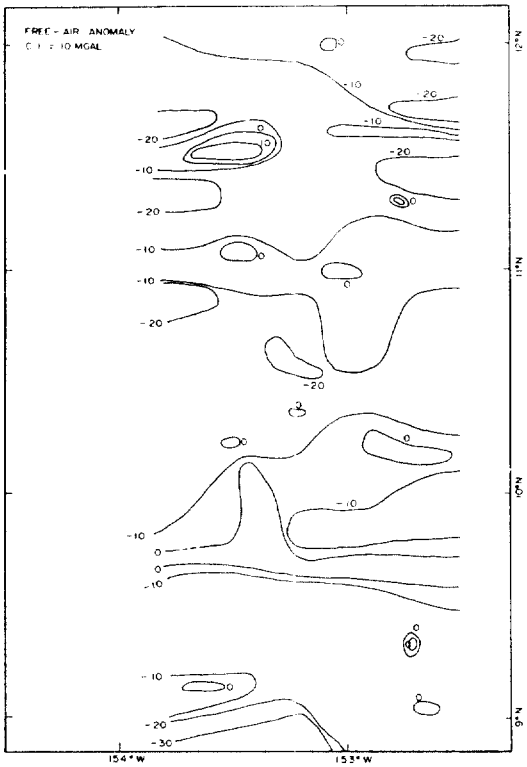

Fig. 4. Contour map of free-air gravity anomaly. Contour interval is 10 mgal.

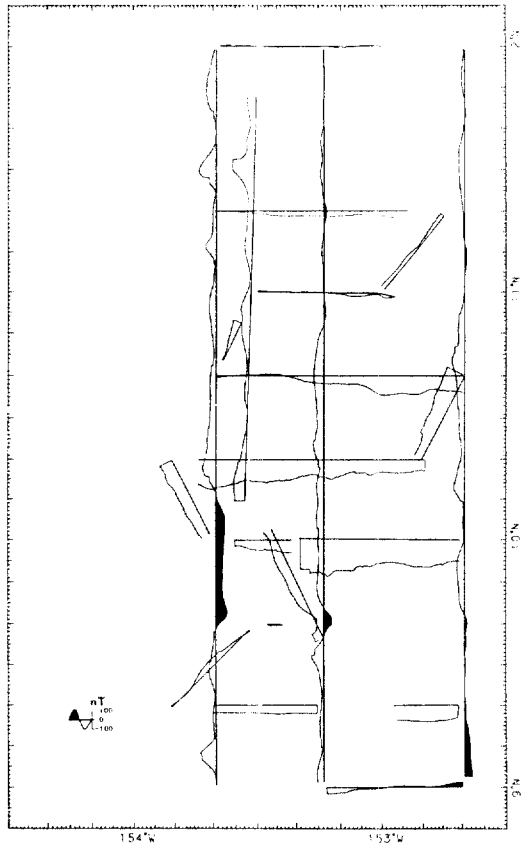

Fig. 5. Magnetic anomaly profiles plotted in a coordinate perpendicular to track lines. Hatched portions denote positive anomaly.

At some cross points, differences of up to 280 nT are found. These crossover errors are attributed mainly to the diurnal variation of geomagnetic field.

To some extent magnetic anomalies reflect the seafloor topography running east west. The amplitude of the magnetic anomalies becomes subdued toward the east just as do changes of seafloor topography.

Fig. 6 compares the magnetic anomaly with the subbottom crustal structure detected by seismic sections. Magnetic anomalies reflect the topographic relief. Negative anomalies occur over most seamounts. An exception is a positive anomaly along the east-west trending seamount chain near 9°40′ N. It is interesting that the seamounts which are offset over 100 km in the east-west direction near 9°40′N have magnetic anomalies of same polarity. This phenomenon would be possible if the seamounts had been formed in several different normal geomagnetic periods. Another explanation for the phenomenon is that the seamounts was formed during one normal geomagnetic period at a position and had been moved west in a left-lateral manner. The latter explanation requires the existence of unknown fractures which cut the east-west trending seamount chain near 9°40′N in the direction of ENE-WSW. The topographic features seems to support the latter explanation as discussed in section of tectonic setting.

In some places, peaks of the negative anomaly do not occur just over seamounts' summits. This phenomenon could be interpreted as the result of the ovelapping of normal polarity of seamounts on an overall positive anomaly of the Mesozoic quiet zone. In some cases, abrupt changes of magnetic intensity are found even though the seafloor

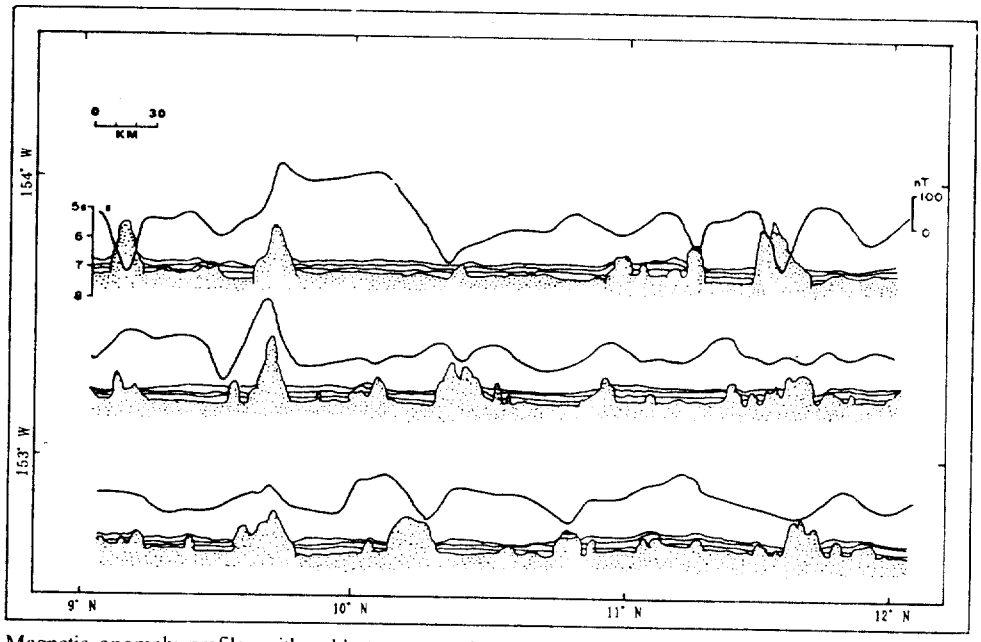

Fig. 6. Magnetic anomaly profiles with subbottom crustal structures. Subbottom crustal structures were drawn from seismic sections.

topography is flat. Seismic interpretation indicates that large amplitude magnetic anomalies, which are not likely related to the topographic features, arise from concealed intrusive masses beneath the seafloor (Fig. 6). Some seamounts have both positive and negative anomalies simultaneously. This phenomenon indicates that those seamounts include different remnant magnetizations.

To review the magnetic anomalies associated with seafloor spreading of the Pacific plate we plotted its residuals after a removal of linear trend from the anomaly profiles of Fig. 5 in the east-west direction. Over the most of oceanic crust in this region, magnetic anomalies are extremely low (−30 to +25 nT) except for some places where the bottom topography is irregular (Fig. 7). Hays and Pitman (1970) suggested that the magnetic quiet zone in the North Pacific is in the area west of anomaly 32. The magnetic quiet zone spans the area between 85 Ma and 110 Ma in age and has a normal magnetic polarity. Park *et al.* (1986) investigated magnetic anomaly profiles around 150° west longitude, west of anomaly 32, and found no magnetic lineations. The facts that no magnetic lineation can be traced over the area and anomalies of small amplitude with no polarity change prevail in the area, support that the oceanic crust of the area was formed during the Cretaceous period.

SEISMIC RESULTS

Features on Sea Bottom and Crustal Structure

The water bottom reflectors are relatively weak in the study area. Sometimes they are not seen with the air-gun single channel seismic data. The weak reflectivity of the sea bottom has been attributed to low density contrast between seawater and unconsolidated sediments. Velocity logs from the DSDP 163 site indicate that the upper 90 m of the sedimentary section has velocities less then 1.6 km/sec (van Andel *et al.*, 1973).

There are many seamounts and intrusive masses within the sedimentary layers of the study area. Dimension of seamounts range from 2.5 to 25 km in basal width and up to 1.9 km in height (Fig. 6). Some seamounts are flanked with moat-like struc-

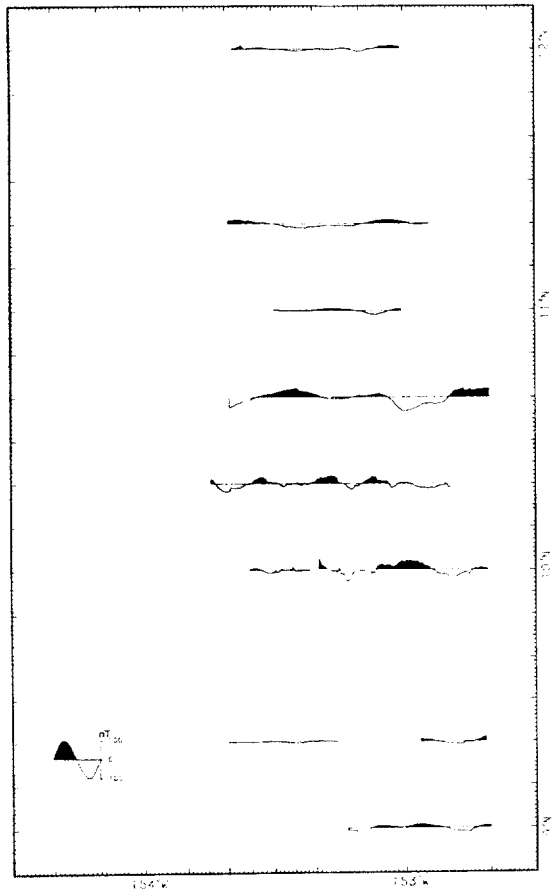

Fig. 7. Residual magnetic anomaly profiles along east-west track lines.

tures at their base (Fig. 8). Existence of undeformed sedimentary layers beneath these moat-like structures suggests that their formation is related to depositional mechaism rather than subbottom movement. Movement of Antarctic Bottom water, flowing from SSW to NNE may be rapid enough to create erosion or non-deposition near the base of the ridges (Holmes and Suk, 1990).

A typical seismic section showing overall crustal structure of the of study area is shown in Fig. 9. The cross section shows seamounts and concealed igneous bodies within the sedimentary section (A & C in Fig. 9). The Age relationship between seamount activity and sedimentary layers can be inferred from the seismic section. The sedimentary layers over rock mass C are folded and include many normal faults and graben structures. This indicates uplifting of rock mass C after the deposition of overlying sedimentary rocks. In particular, the seismic facies of parallel and continuous reflectors with high amplitude of the topmost section of the sedimentary layers over rock mass C indicates the turbidite sequence deposited at a lower place than present place. This supports the fact that volcanic activity occurred recentely in contrast to the general consideration of the area as a tectonically calm area. Seamount B represents volcanic acitivity that occurred at differnt time from the

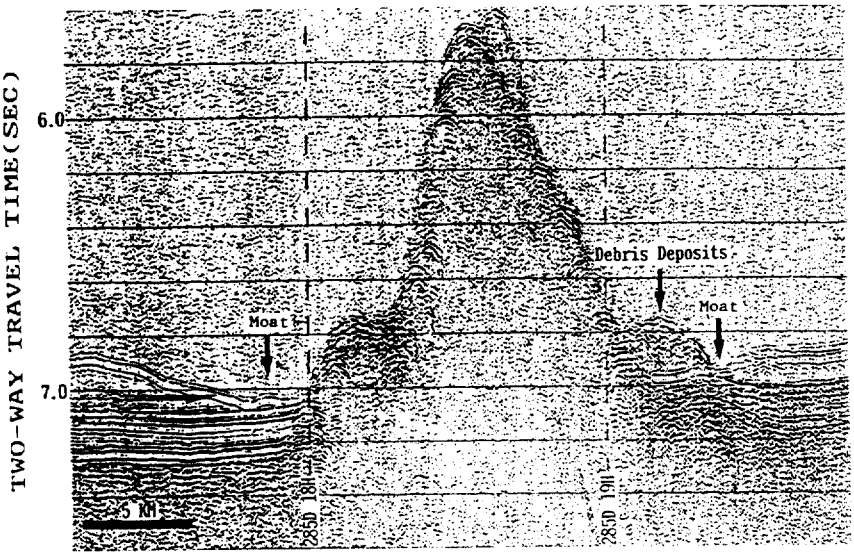

Fig. 8. Seismic section showing geologic features near a seamount. Moat structures and a talus pile are denoted.

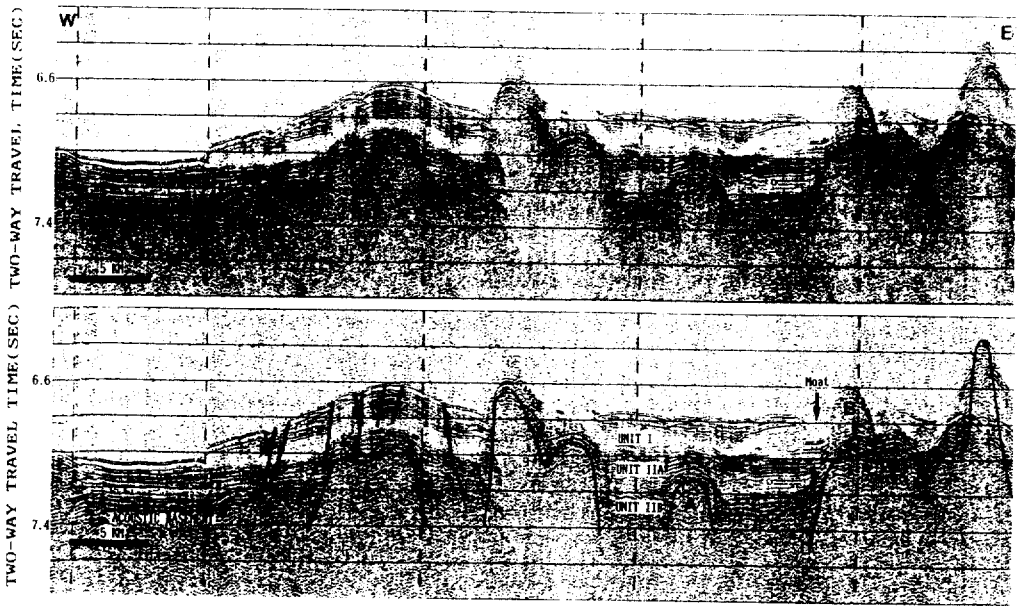

Fig. 9. Uninterpreted and interpreted seismic section of a line shown in Fig. 2.

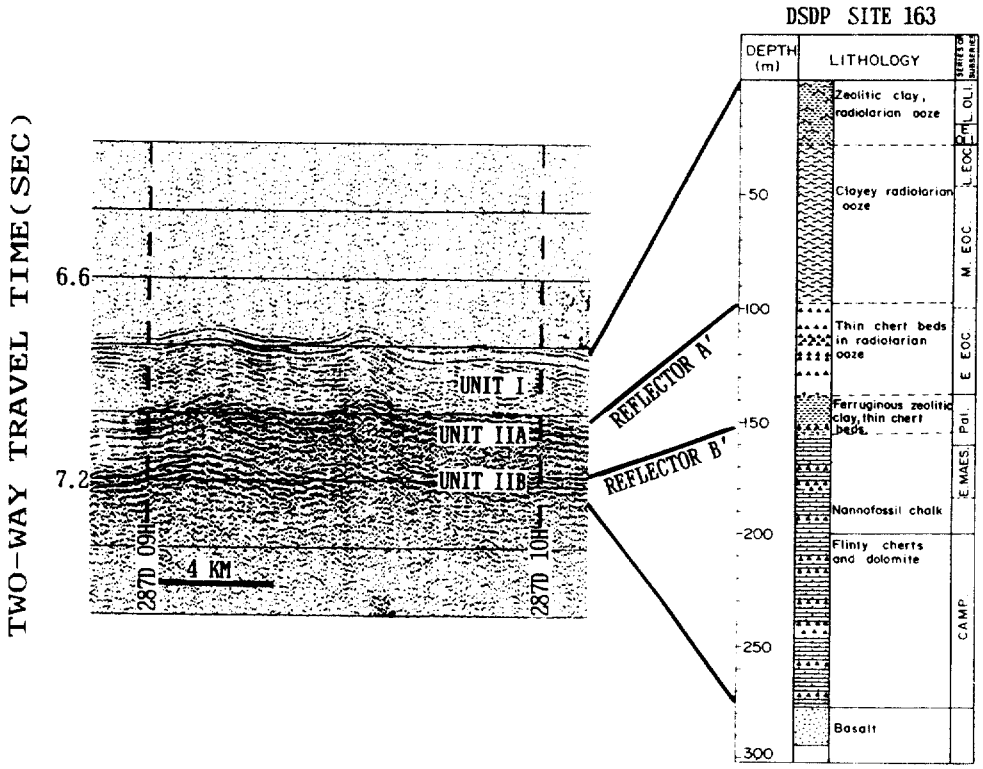

Fig. 10. A typical seismic section showing subdivisions of the sedimentary section of the study area. DSDP 163 data are correlated with the seismic section.

lower main igneous body. The existence of the moat structure in the west of the seamount rules out the possibility of sideswipe from a nearby seamount.

Reflection Characteristics of the Sedimentary Layers

The sedimentary section of the central Pacific ocean basin has been divided into Unit I and Unit II based on reflection characteristics (Ewing *et al.*, 1966; Tamaki, 1977; Tamaki and Tanahashi, 1981; Jeong *et al.*, 1988).

The sedimentary layer of the study area shows a typical seismic reflection pattern of the central Pacific ocean. A typical seismic section of area is correlated with the DSDP 163 data in Fig. 10. The seismically transparent layer at the top is correlated to Unit I of Tamaki and Tanahashi (1981). Unit I is distinguished from the older and more reflective section (Unit II) by a strong refletor (Reflector A'). Correlation of the seismic section with drill data of DSDP 163 indicates that Unit I consists most of unconsolidated clayey ooze and clay (Fig. 10). Unit I has sonic velocities of 1.50 km/sec in average and low bulk densities of 1.14 to 1.26 g/cc (van Andel *et al.*, 1973). Low values of velocities and densities made the Unit I sometimes too transparent to be distinguished from the overlying water layer.

Unit II has usually been divided into two subunits of Unit IIA and Unit IIB by a strong reflector (Reflector B') (Fig. 10). The upper part of Unit IIA, having parallel and continuous reflectors with high amplitude, consists of thin chert beds separated by soft sediment (probably radiolarian ooze) based on the DSDP 163 data (van Andel *et al.*, 1973). Intercalating chert beds and soft sediment layers provide good contrast of acoustic impedance at the chert bed-soft sediment boundary and the acoustic laminations on seismic sections. The seismic transparency of the lower part of Unit IIA is explained by the lack of conspicuous lithologic boundaries. The DSDP 163 data shows that the lithology of this part is mostly ferruginous clay (van Andel *et al.*, 1973).

Unit IIB shows parallel and continuous reflectors with high amplitude along all the seismic profiles. Strong reflectors in this unit inhibit imaging of the basement and estimation of total thickness of sedimentary section. Lithology of the unit consists of intercalating layars of relatively thick chalk and relatively thin chert. Chalk layers and chert layers have sonic velocities of 1.6-1.7 km/sec and about 4.9 km/sec, respectively (van Andel *et al.*, 1973). The good velocity contrast at the lithologic boundary resulted in strong continuous reflectors in the unit.

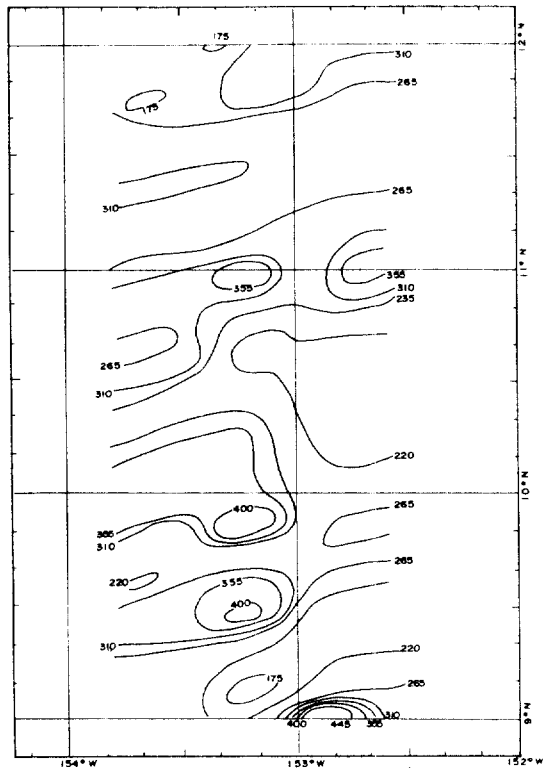

Fig. 11. Isopach map of the study area. Contour values repersent two-way travel time (msec) through the layers of Unit I and Unit IIA.

The basement of the sedimentary section, the top of oceanic crust, is not easily discernible in most of the seismic sections. Diffractions, which are sometimes found below the Unit IIB, are interpreted to be the top of the layer 2 of oceanic crust. The top of the layer 2 is generally understood to have an irregular surface due to volcanic activity which results in diffractions in a seismic

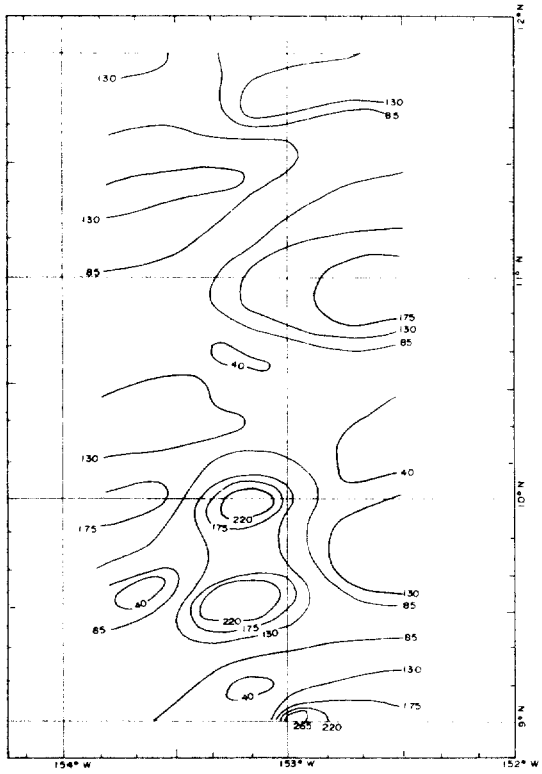

Fig. 12. Isopach map of the Unit I. Contour values represent two-way travel time (msec).

section.

Thickness of Sedimentary Section and Distribution of Manganese Nodules

Fig. 11 shows the total thickness of Unit I and Unit IIA. The sediment layer is thicker in the south where there are more seamounts than in the north. The thickness of sedimentary section is over 280 m south of 10°N and about 140-200 m north of 10°N. Although the thickness of Unit IIB is uncertain due to undicernible basement, a thickness of about 70-100 m in inferred from a seismic section which includes diffractions beneath the Unit IIB (Fig. 9). Therefore, the sedimentary section in the area has a thickness of 200-400 meters.

The relationship between acoustic stratigraphy and abundance and type of manganese nodules has been studied in the Equatorial Central Pacific basin (Price and Calvert, 1970; Piper and Blueford, 1982; Usui and Tanahashi, 1986). The factors which affect growth rate, abundance, and patterns of deposition for manganese nodules are not well understood yet. Interaction of such factors as sediment chemistry, near bottom currents and sedimentary environments have been considered to establish proper conditions for nodule growth and preservation (Holmes and Suk, 1990). A general rule found in previous studies is that nodule abundance is inversely related to the thickness of Unit I where the layer is seismically transparent.

Isopach map of the Unit I (Fig. 12) shows a range of 40-230 msec in two-way travel time, 30-170 m in thickness assuming 1.5 km/sec for the velocity of the layer. The comparison of the isopach contours of the Unit I with the manganese nodule abundances in the study area (Kang *et al.*, 1990; Jung *et al.*, 1990) indicates that manganese nodules are abundant on or around the ridges in the southern part of the area where the Unit I layer is thicker than 130 msec (two way travel time). Relationships between the bottom topography and manganese nodule abundance have been studied in the equatorial north Pacific and central Pacific basins. Rather unusual relationships between sediment thickness and bathymetry were observed at the DOMES site A in the equatorial North Pacific: bathymetric lows of non-deposition and highlands with thick Quaternary sediments. Piper and Blueford (1982) attributed this relationship to erosion of sediments during the past 2×10^6 years by Antarctic Bottom Water through the E-W trending valley in this area. It seems that the same explanation can be used in our study area, about 50 km north of DOMES site A, which shows high manganese nodule abundance on or around the elongated ridges in the south.

SUMMARY AND CONCLUSIONS

We have shown the magnetic and gravity anomaly and seismic reflection profiles. It seems that they can be interpretted in relation to the E-W trending geological structure in this area. There are small free-air gravity anomalies of less than 20 mgal over seamounts and east-west trending

abyssal hills. All the seamounts have local free-air gravity highes and negative residual gravity anomalies. The negative residual gravity anomalies over seamounts may indicat the existence of low density material beneath seamounts compared to surrounding oceanic crust. The seamounts are also characterized by either positive or negative magnetic anomaly. The peaks in magnetic and gravity anomaly are nearly parallel to the E-W bathymetry trend. This rather unexpected E-W trend offset seems to be related to shear stress in the unnamed fracture zone proposed by Sclater *et al* (1971).

Although we do not have enough information to identify the chronological order of the seamounts, seismic profile gives us some clue on the age relation between the seamounts and the oceanic crust in the area. The age of the oceanic crust has been estimated to be approximately 80 My based on the study at the DSDP site 163 about 100 km to the east. Reflection profiles clearly show that some seamounts were formed after deposition of the Unit II sedimentary rock, indicating that the seamounts are younger than 80 My.

The sedimentary section in the study area can be divided into three seismically different units: Unit I, Unit IIA, and Unit IIB. The total thickness of sedimentary section varies from 200 to 400 meters and the sedimentary section is thicker in the southern region of rough topography near the seamount belt than in the northern flat area. The sediment thickness seems to be related to the bathymetry, which, in turn, affects manganese nodule abundance by erosion due to the bottom water flow. Manganese nodules are abundant in the southern part of the study area where ridges are developed and the Unit I layer is thicker than 100 meters.

ACKNOWLEDGEMENT

We are appreciate to many personels who involved in the onboard data acquisition and navigation crew of the USGS research vessel Farnella. The onboard scientists are as follows:

From KORDI: B.C. Suk (Chief scintist), K.Y. Kim, K.S. Jeong, K.Y. Lee, Y.K. Lee, D.H. Shin, H.S. Jeong, Y.S. Euh, S.H. Yang (Yukong Ltd)

From USGS: M. Holmes (Chief scientist), H. Chezar, B. Hall, M. Hamer, K. Knoshita, T. Lorenson, J. Nicholson, L. Webber, H. Williams, R. Rideout, J. Riordan.

Professors Eric Kunze of University of Washington, C. E. Park of Seoul National Univ., and Y.S. Kong of Pusan Fisheries Univ. are appreciated for the review of this manuscript.

REFERENCES

Andrews, J., G. Freiedrich, G. Pautot, W. Pluger, V. Renard, M. Melguen, D. Cronan, J. Craig, M. Hoffert, P. Stoffers, S. Shearme, T. Thijssen, G. Glasby, N. LeNotre, and P. Saget, 1984. The Hawaii-Tahiti tranect: The oceanographic environment of manganese nodule deposits in the central Pacific. *Marine Geology*, **54**: 109-130.

Calbert, S.E., N.B. Price, G.R. Heath and T.C. Moore, Jr., 1978. Relationship between Ferromanganese nodule compositions and sedimentation in a small survey area of the equatorial Pacific. *J. Mar. Res.*, **36**(1): 161-183.

Ewing, M., T. Saito and J.I. Ewing, 1966. Lower Cretaceous sediments from the Northwest Pacific. *Science*, **152**: 751-775.

Hays, D.E., and Pitman, W.C., III. 1970. Magnetic lineations in the North Pacific, in Hays, J. D. ed., Geological investigations of the North Pacific. *Gelo. Soc. America Mem.*, **126**: 291-314.

Holmes, M.L. and B. Suk, 1990. Preliminary cruise report. Research vessel Farnella Fll-89-CP. USGS and KORDI.

Jeong, K.S., S.J. Han and S.R. Kim, 1988. Acoustic stratigraphy and sedimentary processes in the KONOD-1 area between the Clarion and Clipperton frature zones, northeastern equatorial Pacific. *Jour. Ocean. Soc. Korea*, **23**(1): 24-40.

Jung, H.S., K.S. Jeong, K.Y. Lee and J.K. Kang, 1990 Origin of manganese nodules and their distribution in the KODOS-89 area, Northeastern equatorial Pacific. *Jour. Ocean. Soc. Korea*, **25**(4): 189-204.

Kang, J.K. *et al.*, 1990. A study on the strategy for the development of deep seabed mineral resources (II) p.643, BSPG 00094-296-5, Korea Ocean Research and Development Institute.

Larson, R.L., S.M. Smith and C.G. Chase, 1972. Magnetic lineations of Early Cretaceous age in the western equatorial Pacific Ocean. *Earth Planet. Lett.*, **15**: 315-319.

Park, C.H., S.R. Kim, S.J. Han and J.K. Kim, 1986. Interpretation of the magnetic anomalies in the Northeastern Equatorial Pacific (KONOD-1 area). *Ocean Research*, **8**(2): 17-27.

Piper, D.Z. and J.R. Blueford, 1982. Distribution, Minera-

logy, and texture of manganese nodules and their relation to sedimentation at DOMES site A in the equatorial North Pacific. *Deep-Sea Research.* **29**: 927-952.

Price, N.B. and S.E. Calvert, 1970. Compositional Variation in Pacific Ocean ferromanganese nodules and its relationship to sediment accumulation rates. *Marine Geology,* **9**: 145-171.

Sclater, J.G., R.N. Anderson and M.L. Bell, 1971. Elevation of ridges and evolution of the central eastern Pacific. *Jour. Geophys. Res.,* **76**: 7888-7915.

Tamaki, K., 1977. Study on Substrate stratigraphy and structure by continuous seismic reflection profiling survey. *Geological Survey of Japan Cruise Report.* No. **8**: 51-74.

Tamaki, K. and M. Tanahashi, 1981. Seismic reflection survey in the northeastern margin of the Central Pacific Basin. Geological Survey of Japan Cruise Report, No. **15**: 77-99.

Usui, A. and M. Tanahashi, 1986. Relationship between local variation of nodule facies and acoustic stratigraphy in the GH81-4 area. Geological Sociesty of Japan Cruise Report, No. 21: 160-170.

van Andel, T.H., G.R. Heath, *et al.*, 1973. Site 163. Initial reports of the Deep Sea Drilling Project, Vol. 16, Washington (U.S. Government Printing Office): 411-471.

van Andel, T.H. and R. Heath, 1973. Geological results of Leg 16: The central equatorial Pacific West of the East Pacific Rise. Initial reports of the Deep Sea Drilling Project, Volume 16, Washington (U.S. Government Printing Office).

Wessel, P. and A.B. Watts, 1988. On the accuracy of marine gravity measurements. *Jour. Geophys. Res.,* **93** (B1): 393-413.

Winterer, E.L., 1976. Bathymetry and regional tectonic setting of the Line Islands chain. Initial reports of the deep sea drilling project. Vol. 33, Washington (U.S. Government Office): 731-747.

Winterer, E.L. *et al.*, 1973. Site 164. Initial reports of the deep sea drilling project. Vol. 17. Washington (U.S. Government Printing Office).

Received October 8, 1990
Accepted January 30, 1991